Article

The C–H Activation of Methane by Laser-Ablated Zirconium Atoms: CHZrH, the Simplest Carbene Hydride Complex, Agostic Bonding, and (CH)ZrH

Han-Gook Cho, Xuefeng Wang, and Lester Andrews

J. Am. Chem. Soc., **2005**, 127 (1), 465-473• DOI: 10.1021/ja0451259 • Publication Date (Web): 14 December 2004

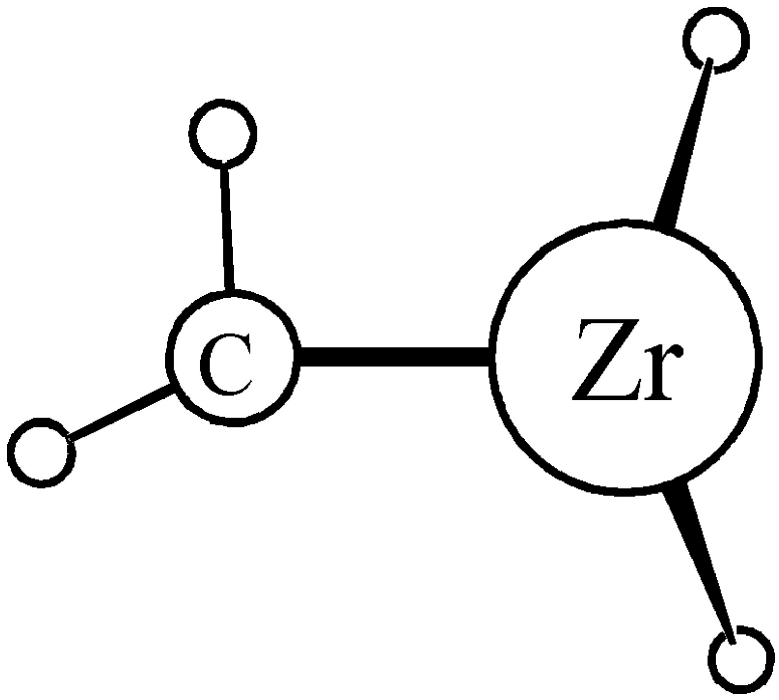

J|A|C|S
ARTICLES
Published on Web 12/14/2004

The C−H Activation of Methane by Laser-Ablated Zirconium Atoms: CH_2═ZrH_2, the Simplest Carbene Hydride Complex, Agostic Bonding, and $(CH_3)_2ZrH_2$

Han-Gook Cho, Xuefeng Wang, and Lester Andrews*

Contribution from the Department of Chemistry, University of Virginia, P.O. Box 400319, Charlottesville, Virginia 22904-4319

Received August 12, 2004; E-mail: lsa@virginia.edu

Abstract: Reaction of laser-ablated Zr with CH_4 ($^{13}CH_4$, CD_4, and CH_2D_2) in excess neon during condensation at 5 K forms CH_2═ZrH_2, the simplest alkylidene hydride complex, which is identified by infrared absorptions at 1581.0, 1546.2, 757.0, and 634.5 cm^{-1}. Density functional theory electronic structure calculations using a large basis set with polarization functions predict a C_1 symmetry structure with agostic C−H- - -Zr bonding and distance of 2.300 Å. Identification of the agostic CH_2═ZrH_2 methylidene complex is confirmed by an excellent match of calculated and observed isotopic frequencies particularly for the four unique CHD═ZrHD isotopic modifications. The analogous reactions in excess argon give two persistent photoreversible matrix configurations for CH_2═ZrH_2. Finally, methane activation by CH_2═ZrH_2 gives the new $(CH_3)_2ZrH_2$ molecule.

Introduction

High oxidation state transition-metal complexes containing a carbon−metal double bond are important for understanding the nature of metal coordination and for developing catalysts in alkene metathesis and alkane activation reactions.[1−3] The activation of methane has always been a challenge to chemists. A number of early transition-metal alkylidenes are agostic,[1] and these compounds provide the opportunity to characterize the agostic interaction of hydrogen to a transition-metal center in a simple carbene complex and to help understand the important alkane C−H bond activation process.[4−8] Most agostic interactions involve much more complicated ligand complexes and a metal cation center. Two tantalum−neopentylidene complexes with short (2.04−2.12 Å) agostic bonds are cases in point.[9] Finally, the selective C−H activation of alkanes by transition-metal catalysts is a major step in the synthesis of useful chemicals.

The simplest compound of this type is the methylidene complex, CH_2═MH_2, which is a six-atom molecule and provides an ideal model system to examine substituent effects and the agostic interaction. Such group 4 compounds have been investigated by early electronic structure calculations using small basis sets and found to have symmetrical structures without agostic interaction.[10,11] Recently, we have reacted laser-ablated Ti, Zr, and Hf atoms with CH_3F and prepared the fluorine substituted CH_2═MHF derivatives.[12−14] These methylidenes result from α-hydrogen migration in the CH_3MF intermediate formed in the initial reaction. It is important that our electronic structure calculations using basis sets with polarization functions reveal a tilted CH_2 group and provide evidence for agostic interaction in these CH_2═MHF molecules.

In the case of Ti, the CH_3TiF insertion product undergoes reversible photochemical rearrangement[12] with CH_2═TiHF and further reaction with CH_3F to form the dimethyl titanium difluoride $(CH_3)_2TiF_2$.[15] In the Zr system, the CH_3ZrF intermediate gives way upon UV irradiation to CH_2═ZrHF, which is believed to execute a persistent, reversible photochemical rearrangement between the ground singlet state and the triplet state.[13] The triplet state has a different structure, which either is captured by the matrix or relaxes to the singlet state with a different argon matrix packing configuration. In the Hf reaction, the CH_3HfF intermediate is not trapped, but its α-H transfer product, the ground singlet CH_2═HfHF carbene complex, is observed and characterized.[14]

The Zr and CH_4 reaction has been investigated by experiment and theory. Klabunde et al. found that thermal Zr atoms do not react with methane,[16] and Bloomberg et al. computed a significant energy for this C−H activation to form CH_3ZrH.[17]

(1) Schrock, R. R. *Chem. Rev.* **2002**, *102*, 145.
(2) Legzdins, P.; Tran, E. *J. Am. Chem. Soc.* **1997**, *119*, 5071.
(3) Buchmeiser, M. R. *Chem. Rev.* **2000**, *100*, 1565.
(4) Crabtree, R. H. *Chem. Rev.* **1985**, *85*, 245.
(5) Crabtree, R. H.; Hamilton, D. G. *Adv. Organomet. Chem.* **1988**, *28*, 299.
(6) Zhang, K.; Gonzalez, A. A.; Mukerjee, S. L.; Chou, S.-J.; Hoff, C. D.; Kubat-Martin, K. A.; Barnhart, D.; Kubas, G. J. *J. Am. Chem. Soc.* **1991**, *113*, 9170.
(7) Ujaque, G.; Cooper, A. C.; Maseras, F.; Eisenstein, O.; Caulton, K. G. *J. Am. Chem. Soc.* **1998**, *120*, 361.
(8) Wada, K.; Craig, B.; Pamplin, C. B.; Legzdins, P.; Patrick, B. O.; Tsyba, I.; Bau, R. *J. Am. Chem. Soc.* **2003**, *125*, 7035.
(9) Schultz, A. J.; Brown, R. K.; Williams, J. M.; Schrock, R. R. *J. Am. Chem. Soc.* **1981**, *103*, 169.
(10) (a) Franci, M. M.; Pietro, W. J.; Hout, R. F., Jr.; Hehre, W. J. *Organometallics* **1983**, *2*, 281. (b) Franci, M. M.; Pietro, W. J.; Hout, R. F., Jr.; Hehre, W. J. *Organometallics* **1983**, *2*, 815.
(11) Cundari, T. R.; Gordon, M. S. *J. Am. Chem. Soc.* **1992**, *114*, 539.
(12) Cho, H.-G.; Andrews, L. *J. Phys. Chem. A* **2004**, *108*, 6294.
(13) Cho, H.-G.; Andrews, L. *J. Am. Chem. Soc.* **2004**, *126*, 10485.
(14) Cho, H.-G.; Andrews, L. *Organometallics* **2004**, *23*, 4357.
(15) Cho, H.-G.; Andrews, L. *Inorg. Chem.* **2004**, *43*, 5253.

Like CH_3ZrF, it is expected that CH_3ZrH will undergo α-H transfer to form the simplest carbene hydride complex, $CH_2{=}ZrH_2$. Fortunately, the methylidene $CH_2{=}ZrH_2$ contains two intense infrared chromophores, namely the CH_2 and ZrH_2 groups, which are sensitive to the distortion associated with intramolecular agostic bonding. Hence, the infrared spectrum of $CH_2{=}ZrH_2$ can provide evidence for agostic interaction through symmetry lowering in the molecule and from computations using large basis sets. In particular, the number of CHD=ZrHD isotopomers so formed provides a ready method to verify agostic interaction in this simplest carbene hydride complex as only two isotopomers (cis and trans) will be formed if there is no agostic interaction (symmetric CH_2 group in C_s or C_{2v} symmetry), but four isotopomers (cis and trans for H and for D in the agostic position) if there is agostic interaction (asymmetric CH_2 group in C_1 symmetry). We describe the first experimental characterization of the simplest alkylidene hydride complex, $CH_2{=}ZrH_2$, zirconium methylidene, and demonstrate the agostic C−H- - -Zr interaction from the matrix infrared spectra and density functional structure and frequency calculations. A brief report on this work has appeared.[18]

Experimental and Computational Methods

The laser-ablation matrix-infrared experiment has been described previously.[19,20] Briefly, laser-ablated zirconium atoms (Johnson-Matthey) were reacted with CH_4 (Matheson, UHP grade), $^{13}CH_4$, CD_4, and CH_2D_2 (Cambridge Isotopic Laboratories) in excess neon (Spectra Gases) or argon (MG Industries) during condensation on a CsI window at 5 or 8 K. Infrared spectra were recorded at 0.5 cm^{-1} resolution on Nicolet Magna spectrometers with HgCdTe detectors. Samples were irradiated by a mercury arc lamp (175 W, globe removed) for 20 min periods and were annealed, and more spectra were recorded.

Complementary density functional theory (DFT) calculations were done using the Gaussian 98 package,[21] B3LYP density functional, 6-311++G(3df, 3pd) basis sets for C, H, and SDD effective core potential and basis set for Zr (12 valence electrons) to provide a consistent set of vibrational frequencies for the reaction products. Geometries were fully relaxed during optimization, and the optimized geometry was confirmed via vibrational analysis. All the vibrational frequencies were calculated analytically.

Results

Reactions of laser-ablated zirconium and methane in excess argon and neon will be examined, and electronic structure calculations of potential product molecules will be described.

Argon. An extensive investigation of the Zr and CH_4 reaction has been done using 0.2, 0.5, 2, and 5% CH_4 in excess argon.

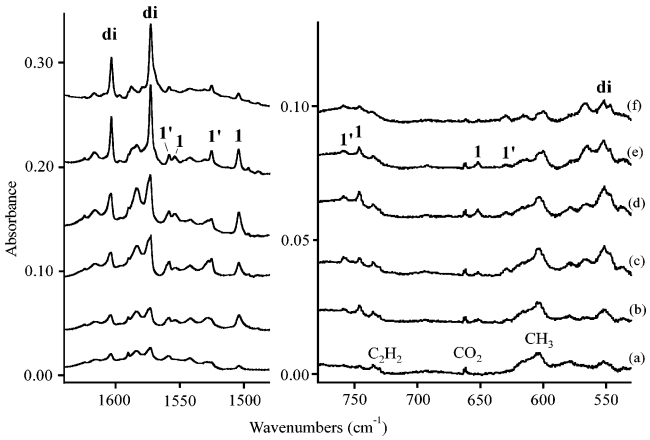

Figure 1. Infrared spectra in the 1620−1480 and 800−500 cm^{-1} regions for laser-ablated Zr co-deposited with 5% CH_4 in argon at 10 K. Spectrum (a) after sample deposition for 60 min, (b) after $\lambda > 530$ nm irradiation, (c) after 240−380 nm irradiation, (d) after $\lambda > 530$ nm irradiation, (e) after annealing to 20 K, and (f) after annealing to 28 K.

The primary product yield increased with reagent concentration, and spectra from the 5% CH_4 experiment are illustrated in Figure 1. Three sets of product absorptions are found in the Zr−H stretching region. The bands at 1504.3, 1553.9 cm^{-1} and at 1524.8, 1557.8 cm^{-1} (marked 1 and 1′) are photoreversible with $\lambda > 530$ nm and $240 < \lambda < 380$ nm radiation. The spectra in Figure 1 show this cycle, which was repeated up to four times in other experiments. The bands at 1572.6 and 1603.1 cm^{-1} (marked di) sharpen and increase on irradiation and on annealing. The di band yield relative to 1 and 1′ absorptions increased markedly with increasing CH_4 concentration. Weaker bands at 1371.1, 1121.0 cm^{-1} are associated with the stronger di bands on photolysis and annealing. The lower frequency region also reveals analogous photoreversible 747.1 and 652.6 cm^{-1} (marked 1) and 759.8 and 630.2 cm^{-1} (marked 1′) absorptions and a weak 552 cm^{-1} band (marked di).

Two experiments were done for each of the $^{13}CH_4$, CD_4, and CH_2D_2 isotopic modifications, and the observed frequencies are listed in Table 1. The $^{13}CH_4$ precursor gave the same absorptions in the upper region, but shifts were found in the lower region. The CD_4 substitution produced large shifts for all product absorptions, and the spectra behaved similarly on photolysis and annealing. Figure 2 shows spectra for the CD_4 reaction.

Perhaps the most important diagnostic information comes from the results of CH_2D_2 substitution. Figure 3 compares spectra of CH_2D_2 reaction products in the Zr−H and Zr−D stretching regions. Although the spectra are complicated by 1 and 1′ absorptions in each region, new absorptions are observed for mixed H, D counterparts for each photochemical product in each region, and these new bands are marked by arrows. Note that two new mixed isotopic bands are observed for 1 and 1′, but only one new mixed H, D band is observed for the di species in each region at 1587.6 and 1140.0 cm^{-1}.

One experiment was performed with a 2% CH_4 plus 2% CD_4 mixture to explore the secondary reaction mechanism. The 1 and 1′ absorptions were observed just as in the CH_4 or CD_4 experiments described above with no isotopic mixing. The di bands at 1603.1, 1572.6, 1147.8, and 1131.8 cm^{-1} were also observed, but in addition new intermediate absorptions were observed with significant intensity at 1587.8 and 1140.6 cm^{-1}.

(16) (a) Klabunde, K. J.; Tanaka, Y. *J. Am. Chem. Soc.* **1983**, *105*, 3544. (b) Klabunde, K. J.; Jeong, G. H.; Olsen, A. W. In *Selective Hydrocarbon Activation: Principles and Progress*; Davies, J. A., Watson, P. L., Greenberg, A., Liebman, J. F., Eds.; VCH Publishers: New York, 1990; pp 433−466.
(17) Bloomberg, M. R. A.; Siegbahn, P. E. M.; Swensson, M. *J. Am. Chem. Soc.* **1992**, *114*, 6095.
(18) Andrews, L.; Cho, H.-G.; Wang, X. *Angew. Chem.* **2005**, *117*, 115.
(19) Chertihin, G. V.; Andrews, L. *J. Phys. Chem.* **1995**, *99*, 6356 (ZrO_2).
(20) Andrews, L.; Citra, A. *Chem. Rev.* **2002**, *102*, 885 and references therein.
(21) Frisch, M. J.; Trucks, G. W.; Schlegel, H. B.; Scuseria, G. E.; Robb, M. A.; Cheeseman, J. R.; Zakrzewski, V. G.; Montgomery, J. A., Jr.; Stratmann, R. E.; Burant, J. C.; Dapprich, S.; Millam, J. M.; Daniels, A. D.; Kudin, K. N.; Strain, M. C.; Farkas, O.; Tomasi, J.; Barone, V.; Cossi, M.; Cammi, R.; Mennucci, B.; Pomelli, C.; Adamo, C.; Clifford, S.; Ochterski, J.; Petersson, G. A.; Ayala, P. Y.; Cui, Q.; Morokuma, K.; Rega, N.; Salvador, P.; Dannenberg, J. J.; Malick, D. K.; Rabuck, A. D.; Raghavachari, K.; Foresman, J. B.; Cioslowski, J.; Ortiz, J. V.; Stefanov, B. B.; Liu, G.; Liashenko, A.; Piskorz, P.; Komaromi, I.; Gomperts, R.; Martin, R. L.; Fox, D. J.; Keith, T.; Al-Laham, M. A.; Peng, C. Y.; Nanayakkara, A.; Challacombe, M.; Gill, P. M. W.; Johnson, B. G.; Chen, W.; Wong, M. W.; Andres, J. L.; Gonzalez, C.; Head-Gordon, M.; Replogle, E. S.; Pople, J. A. *Gaussian 98*, revision A.11.4; Gaussian, Inc.: Pittsburgh, PA, 2002.

Table 1. Infrared Absorptions (cm^{-1}) Observed for Laser-Ablated Zr Atom Reactions with Methane in Excess Neon and Argon

neon					argon					
CH_4	$^{13}CH_4$	CD_4	CH_2D_2	CH_2D_2	CH_4	$^{13}CH_4$	CD_4	CH_2D_2	CH_2D_2	ident.
1617.2	1617.2	1158.1	1616.2	–	1603.1	1603.1	1147.8	1603.1	1148.4	$(CH_3)_2ZrH_2$
			1602.2	1150.5				1587.6	1140.0	Me_2ZrHD
1587.5	1587.5	1142.6	1587.5	1142.5	1572.6	1572.6	1131.8	1572.4	1131.5	$(CH_3)_2ZrH_2$
1586 sh	1586 sh	1136.9			1557.8	1557.8	1115.3	1557.9	1115.1	$CH_2{=}ZrH_2$[a]
1581.0	1581.0	1133.1	1580.7	1132.7	1553.9	1553.9	1111.3	1551.1	1111.9	$CH_2{=}ZrH_2$
1551.0	1551.0	1115.2	1550.1	1115.5	1524.8	1524.8	1097.3	1524.2[e]	1096.8[g]	$CH_2{=}ZrH_2$[a]
1546.2	1546.2	1112.3	1545.5[b]	1112.5[c]	1504.3	1504.3	1082.4	1503.8[d]	1082 sh	$CH_2{=}ZrH_2$
1533.5	1533.5	1096.8	1533.2	–[f]	1496.2	1496.2	1077.1	1496.1	–[f]	(CH_3ZrH)
					1488.4	1488.4	1071.7	1488.1	–[f]	(CH_3ZrH)
1375.1	1372.0	1009.0	1329.2		1371.1	1367.8		1324.6		$(CH_3)_2ZrH_2$
1125.0	1114.8	895.9	949.4		1121.0	1111.0	893			$(CH_3)_2ZrH_2$
					759.8		694.6	755	721	$CH_2{=}ZrH_2$[a]
757.0	737.4	687.0	750	718	747.1	731.1	668.7	733	702	$CH_2{=}ZrH_2$
					652.6	648.2	524.6	627	527	$CH_2{=}ZrH_2$[a]
634.5	629.8	499.4			630.2	625.6	497.1	591	551[h]	$CH_2{=}ZrH_2$
593.4	592.2	–								$(CH_3)_2ZrH_2$
564.2	559.2	469.7			552		467.3			$(CH_3)_2ZrH_2$

[a] Absorptions due to different neon or argon packing configuration (marked 1′ in the figures). [b] Additional bands at 1554.4 and 1571.0 cm^{-1} with annealing counterparts at 1558.7 and 1573.3 cm^{-1} for CHD═ZrHD isotopomers. [c] Additional bands at 1116.2 and 1129.2 cm^{-1} with annealing counterparts at 1118.9 and 1133.0 cm^{-1} for CHD═ZrHD isotopomers. [d] Additional bands at 1517.0, 1531.0 cm^{-1}. [e] Additional bands at 1535.1, 1543.5 cm^{-1}. [f] Masked by CH_2D_2 precursor. [g] Additional bands at 1105.9, 1110.9 cm^{-1}. [h] Additional bands at 558, 524, and 518 cm^{-1}.

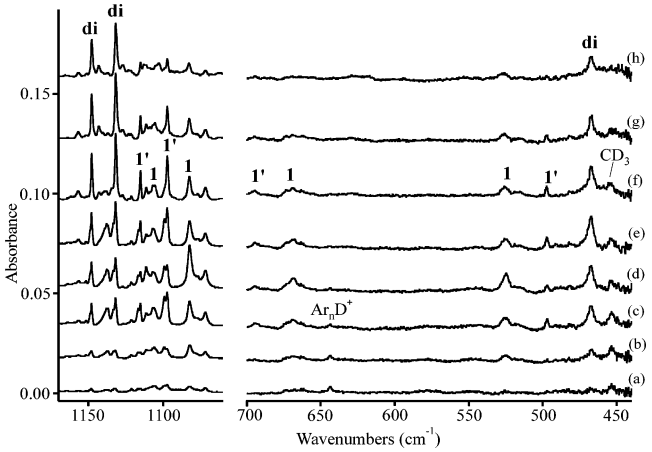

Figure 2. Infrared spectra in the 1170−1060 and 700−440 cm^{-1} regions for laser-ablated Zr co-deposited with 2% CD_4 in argon at 8 K. Spectrum (a) after sample deposition for 60 min, (b) after $\lambda > 530$ nm irradiation, (c) after 240−380 nm irradiation, (d) after $\lambda > 530$ nm irradiation, (e) after 240−380 nm irradiation, (f) after annealing to 20 K, (g) after annealing to 26 K, and (h) after annealing to 32 K.

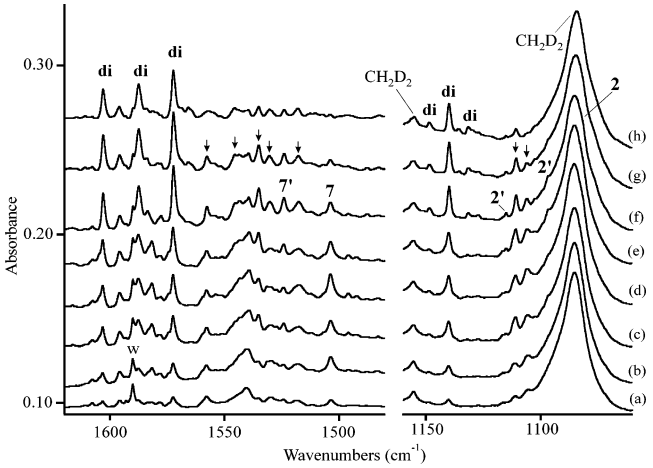

Figure 3. Infrared spectra in the 1620−1480 and 1160−1060 cm^{-1} regions for laser-ablated Zr co-deposited with 1% CH_2D_2 in argon at 8 K. Spectrum (a) after sample deposition for 60 min, (b) after $\lambda > 530$ nm irradiation, (c) after 240−380 nm irradiation, (d) after $\lambda > 530$ nm irradiation, (e) after 240−380 nm irradiation, (f) after annealing to 20 K, (g) after annealing to 26 K, and (h) after annealing to 32 K.

Neon. The Zr and CH_4 reaction in excess neon gives fewer product absorptions on sample deposition, and the primary product yield is less because it is necessary to use lower laser energy in order to isolate reaction products in solid neon. Infrared spectra are illustrated in Figure 4 in the Zr−H stretching region for laser-ablated Zr and CH_4 (0.4% in neon). Four new product absorptions are observed at 1546.2 and 1581.0 cm^{-1} (labeled 1) and at 1587.5 and 1617.2 cm^{-1} (labeled di). The bands increased on $\lambda > 530$ nm and 240−380 nm irradiations. Annealing to 10 K sharpened and slightly increased these absorptions and produced a new 1551.0 cm^{-1} satellite feature. Further annealing to 11 K increased the 1587.5, 1617.2 cm^{-1} set, decreased the 1546.2, 1581.0 cm^{-1} pair, and increased the satellite. Continued annealing to 12 K increased the upper set another 10%, almost destroyed the lower pair, markedly increased the 1551.0 cm^{-1} satellite and an associated 1586 cm^{-1} shoulder absorption. Subsequent visible and UV irradiation decreased the 1586, 1551.0 cm^{-1} features in favor of the original 1581.0 and 1546.2 cm^{-1} bands and slightly decreased the 1617.2 and 1587.5 cm^{-1} absorptions. A similar experiment with 0.2% CH_4 in neon gave weaker product absorptions, particularly for the di bands, and the same photolysis and annealing behavior.

Table 1 lists these frequencies, their unshifted $^{13}CH_4$ counterparts, and similar displaced CD_4 reaction product bands. Figure 5 compares spectra in the Zr−H and Zr−D stretching regions for reactions with CH_4, CH_2D_2, and CD_4. The important new information is that two new mixed H, D absorptions (marked 4,6 and 3,5) appear between the lower pair in each region, and one new mixed H, D band (marked di) appears between the upper pair in each region. Note that the di bands increase markedly on annealing.

The lower frequency region contains four associated weaker absorptions at 757.0, 634.5, 593.4, and 564.2 cm^{-1}. The first two track on photolysis and annealing with the lower pair in the Zr−H stretching region, and the 593.4 and 564.2 cm^{-1} absorptions follow the 1617.2, 1587.5 cm^{-1} pair. A weak 1375.1 cm^{-1} band and the 1125.0 cm^{-1} absorption (Figure 5f) also

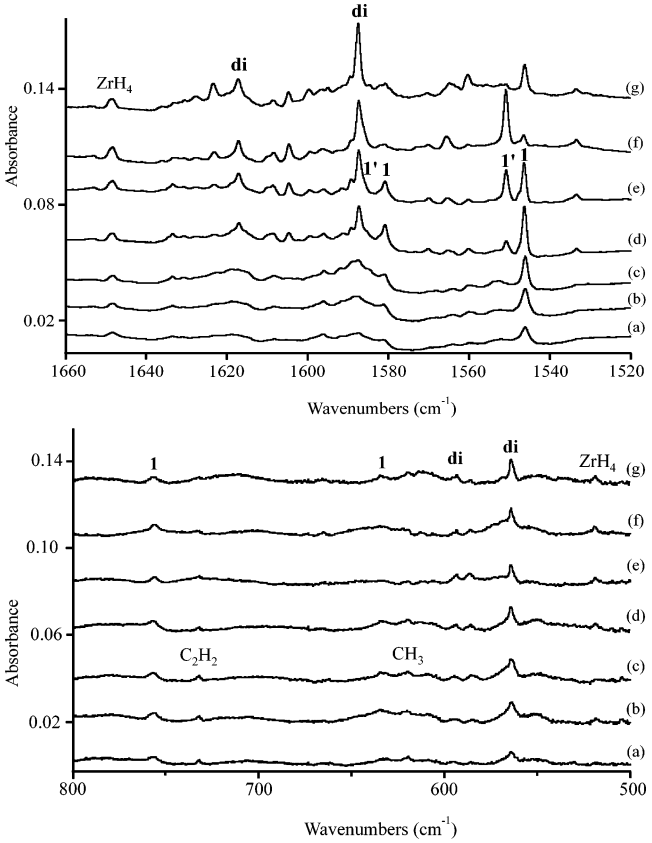

Figure 4. Infrared spectra in the 1660−1520 and 800−500 cm^{-1} regions for laser-ablated Zr co-deposited with CH_4 in excess neon at 5 K. 0.4% CH_4 (a) in neon deposited for 45 min, (b) after $\lambda > 530$ nm irradiation for 20 min, (c) after 240−380 nm irradiation for 20 min, (d) after annealing to 10 K, (e) after annealing to 11 K, (f) after annealing to 12 K, and (g) after $\lambda > 220$ nm irradiation.

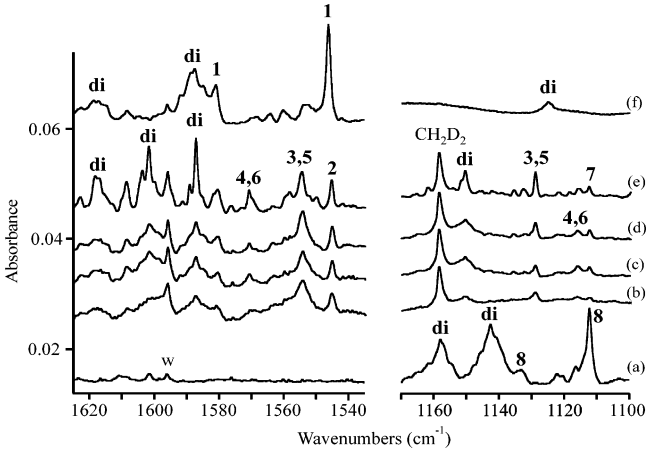

Figure 5. Infrared spectra in the Zr−H and Zr−D stretching regions for laser-ablated Zr co-deposited with CH_4, CH_2D_2, and CD_4 in excess neon at 5 K. (a) 0.4% CD_4 in neon after $\lambda > 530$ and 240−380 nm irradiations, (b) 0.6% CH_2D_2 in neon, (c) after 240−380 nm irradiation, (d) after $\lambda > 530$ nm irradiation, (e) after annealing to 11 K, and (f) 0.4% CH_4 in neon after $\lambda > 530$ and 240−380 nm irradiations.

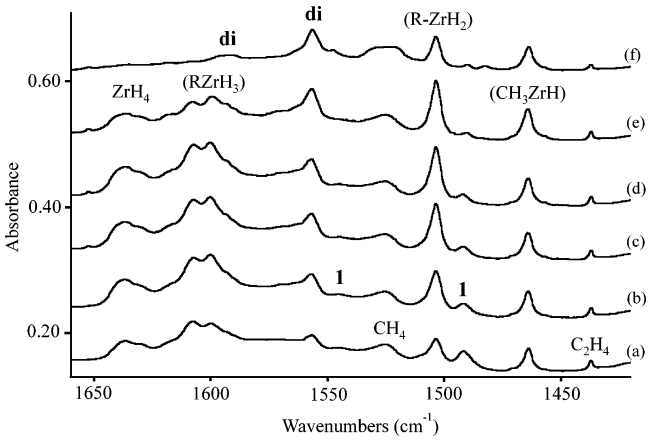

Figure 6. Infrared spectra in the 1660−1420 cm^{-1} region for laser-ablated Zr co-deposited with pure CH_4 at 8 K. Spectrum (a) after sample deposition for 30 min, (b) after $\lambda > 530$ nm irradiation, (c) after 240−380 nm irradiation, (d) after $\lambda > 530$ nm irradiation, (e) after annealing to 20 K, and (f) after annealing to 32 K. Parentheses indicate tentative identifications.

track with the di group. The $^{13}CH_4$ and CD_4 isotopic counterparts are given in Table 1.

Methane. Two experiments were performed using pure CH_4 or CD_4 as the matrix in attempt to learn more about Zr−CH_4 chemistry under high methane concentration conditions. Spectra from the CH_4 investigation are illustrated in Figure 6. The major absorptions produced on sample deposition at 1503 and 1464 cm^{-1} increased and then decreased during the irradiation and annealing cycles, while minor 1557 and 547 cm^{-1} bands increased steadily, 1545 and 1492 cm^{-1} absorptions decreased stepwise, and broad 1637, 1608, 1600 cm^{-1} absorption decreased through this procedure. New absorptions at 3270, 736 cm^{-1}, at 1437, 950 cm^{-1}, and at 822 cm^{-1} are due to the stable C_2H_2, C_2H_4, and C_2H_6 molecules made by fragmentation of methane exposed to irradiation in the laser-ablation process.[22−24] The deuterium counterparts were observed at 2426, 542 cm^{-1}, at 1069, 722 cm^{-1}, and at 595 cm^{-1}. A strong 608.6 cm^{-1} absorption decreased on annealing and is probably due to the CH_3 radical trapped in solid methane: The deuterium species shifted to 458.9 cm^{-1}. These bands were observed at 603 and 453 cm^{-1} in solid argon.[25]

Calculations. Calculations were performed for $CH_2{=}ZrH_2$ using the B3LYP density functional, and the global minimum energy C_1 structure with no symmetry is illustrated in Figure 7. This fully relaxed molecule with no imaginary frequencies is clearly distorted at both C and Zr centers. Note that the longer C−H bond and the shorter Zr−H bond are cis to each other. The CH_2 group is tilted owing to the agostic C−H- - -Zr interaction. Additional calculations using the BPW91 functional and the MP2 method[21] gave similar skewed structures. The symmetry was fixed at C_s, and this structure with equivalent C−H bonds and Zr−H bonds and one imaginary frequency is 0.01 kcal/mol higher in energy. This structure is not stable and will relax along the imaginary CH_2 rocking mode to the stable C_1 structure. The C_{2v} symmetry was imposed, and this planar structure with two imaginary frequencies is 0.8 kcal/mol higher in energy. Clearly, the C_{2v} form is unstable and will relax along the imaginary CH_2 rocking and ZrH_2 wagging motions to the stable C_1 structure.

The C−H- - -Zr distance computed here, 2.300 Å using the large 6-311++G(3df, 3dp) basis set, is slightly longer than agostic bonds measured for Cr and W complexes in crystals (2.24 and 2.27 Å),[6] but shorter than the agostic bond length

(22) Wang, X.; Andrews, L. *J. Phys. Chem. A* **2003**, *107*, 337.
(23) Cho, H.-G.; Andrews, L. *J. Phys. Chem. A* **2004**, *108*, 3965.
(24) Davis, S. R.; Andrews, L. *J. Am. Chem. Soc.* **1987**, *109*, 4768.
(25) Jacox, M. E. *J. Mol. Spectrosc.* **1977**, *66*, 272.

Table 2. Harmonic Vibrational Frequencies (cm^{-1}) Computed for the C_1 Ground State Structure of $CH_2{=}ZrH_2$ Using Medium and Large Basis Sets

mode	6-311++G(2d,p)		6-311++G(3df,3pd)		6-311++G(3df,3pd)		6-311++G(3df,3pd)	
description	freq.[a]	int.[b]	freq.[a]	int.[b]	freq.[c]	int.[b]	freq.[d]	int.[b]
CH_2 str	3171.8	(1)	3178.8	(1)	2350.9	(3)	3168.1	(1)
CH_2 str	2875.6	(6)	2857.5	(5)	2080.1	(2)	2850.9	(6)
ZrH_2 str	1640.4	(303)	1633.7	(301)	1160.2	(161)	1633.7	(301)
ZrH_2 str	1619.3	(574)	1603.0	(544)	1143.2	(273)	1603.0	(544)
CH_2 scis	1315.7	(17)	1320.1	(16)	1020.8	(21)	1312.1	(16)
C=Zr str	762.2	(134)	766.7	(130)	682.4	(74)	748.7	(134)
CH_2 wag	661.1	(151)	664.7	(144)	520.8	(104)	659.0	(139)
ZrH_2 scis	643.3	(91)	641.6	(85)	463.4	(52)	639.4	(79)
ZrH_2 rock	519.5	(9)	514.8	(10)	385.0	(7)	512.7	(10)
CH_2 twist	415.0	(22)	408.0	(23)	289.1	(12)	407.9	(23)
CH_2 rock	278.3	(131)	309.7	(75)	223.8	(33)	309.2	(77)
ZrH_2 wag	227.0	(95)	239.8	(131)	175.8	(72)	239.1	(129)

[a] $^{12}CH_2{=}ZrH_2$. [b] Infrared intensities (km/mol). [c] $CD_2{=}ZrD_2$. [d] $^{13}CH_2{=}ZrH_2$.

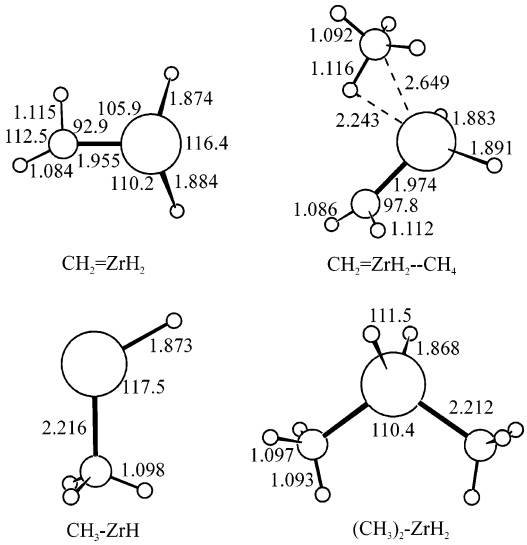

Figure 7. Minimum energy structures computed for $CH_2{=}ZrH_2$, $CH_2{=}ZrH_2$- - -HCH_3, CH_3ZrH, and $(CH_3)_2ZrH_2$ at the B3LYP/6-311++G-(3df,3pd)/SDD level of theory. Bond lengths (Å) and angles (°).

computed (2.379 Å) for a model Ir complex using basis sets with polarization functions.[7] Since agostic bond energies in the 10−15 kcal/mol range have been determined for the group 6 complexes,[6] our slightly longer agostic bond in $CH_2{=}ZrH_2$ is probably almost as strong.

The frequencies calculated for the C_1 $CH_2{=}ZrH_2$ structure are given in Table 2 for two basis sets. The frequencies change from 2 to 18 cm^{-1} with more polarization functions, but the isotopic shifts for the larger basis set fit our experimental results slightly better so we believe the larger basis gives a more accurate vibrational potential function. Accordingly, we list and discuss isotopic data from calculations using the 6-311++G(3df, 3pd) basis set for C, H, and SDD ECP for Zr. The $^{13}CH_2{=}ZrH_2$ and $CD_2{=}ZrD_2$ isotopic modifications are also given in Table 2, along with approximate mode descriptions and infrared intensities. Only four of these absorptions are observable in our experiments. The frequencies and intensities for the six dideuterio isotopic modifications shown in Chart 1 are given in Table 3.

The first computations on $CH_2{=}ZrH_2$ employed the STO-3G minimal basis set and found a planar, symmetrical molecule.[10] Later calculations used the 3-21G basis on C and H with an ECP for Zr and still determined a C_{2v} structure for $CH_2{=}$

Chart 1

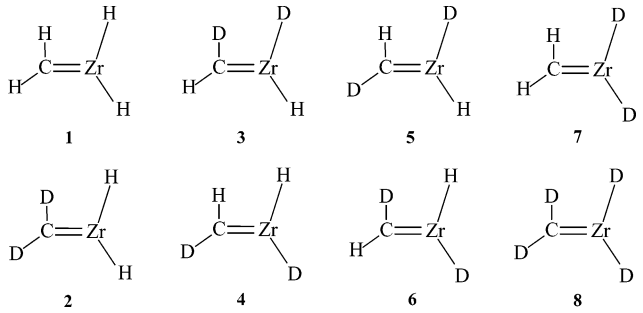

ZrH_2.[11] We performed calculations to find the necessary basis functions to allow distortion of the CH_2 and ZrH_2 subgroups in $CH_2{=}ZrH_2$. The 3-21G basis on C and H and CEP-31G effective core potential and basis on Zr gave a C_s symmetry molecule (∠HCZr, 123.2°; C=Zr, 1.991 Å) with coplanar $H_2C{=}$Zr and two identical out-of-plane H bonds to Zr. This structure is similar to that reported by Cundari and Gordon except for the wagging distortion of ZrH_2. Calculation using 6-311G and the SDD effective core potential gave almost the same structure (Table 4), and the addition of diffuse functions on C and H, 6-311++G, made no difference. However, the 6-311+G(2d) set with diffuse and polarization functions on carbon (not H) gave CH_2 distortion (∠HCZr, 97.1°; C=Zr, 1.963 Å) and C−H- - -Zr distance of 2.373 Å. The addition of a diffuse function on H had no effect (Table 4), but more polarization functions on C reduces the calculated C=Zr and C−H- - -Zr bond distances. The addition of a polarization function on H reduces the agostic bond slightly to 2.345 Å, and the addition of polarization functions to the Zr ECP to balance the basis set appears to have little effect on the structure. It appears that polarization functions on C are more important than those on H. Using the 6-311++(3df,3pd) basis set with four sets of polarization functions on C and H gives a still stronger agostic interaction (∠HCZr, 92.1°; C=Zr, 1.955 Å; C−H- - -Zr, 2.300 Å). As found by previous researchers,[7] polarization functions on C and H are necessary to characterize the agostic interaction. The higher binding energy computed at the 6-311++G(3df,-3pd) level, 21.7 kcal/mol, as compared to the G-311++G(2d,p) level, 21.3 kcal/mol, can be attributed at least partly to a better description of the agostic interaction with more polarization functions. Finally, we repeat the large basis set calculations using the LANL2DZ effective core potential and basis for Zr and find a slightly stronger agostic interaction for $CH_2{=}ZrH_2$ (Table 4).

Table 3. Strongest Infrared Absorptions (cm^{-1}) Calculated for Dideuterio Zirconium Methylidene Isotopic Molecules (Chart 1)[a]

2	3	4	5	6	7
CH_2═ZrD_2	CHD═ZrHD	CDH═ZrDH	CDH═ZrHD	CHD═ZrDH	CD_2═ZrH_2
1160.2 (161)[b]	1610.8 (423)	1625.5 (404)	1610.9 (424)	1625.5 (403)	1633.7 (302)
1143.3 (269)	1161.4 (45)	1193.5 (21)	1193.2 (14)	1161.3 (22)	1602.9 (542)
758.5 (89)	1157.4 (201)	1146.5 (221)	1157.5 (221)	1146.7 (229)	1020.9 (22)
661.7 (146)	754.7 (100)	717.9 (113)	716.1 (105)	753.2 (99)	702.1 (147)
471.3 (40)	643.7 (148)	610.0 (25)	560.8 (61)	647.5 (115)	629.5 (19)
418.5 (10)	548.7 (56)	560.3 (148)	543.9 (122)	609.1 (86)	531.9 (153)
16.930[c]	17.666	17.589	17.520	17.733	18.298

[a] 6-311++G(3df, 3pd) basis set. [b] Infrared intensities (km/mol). [c] Zero point energy, kcal/mol.

Table 4. Structural Parameters (deg, Å) for CH_2═ZrH_2 Calculated with Different Basis Sets at the B3LYP Level of Theory

basis set	∠H–C–Zr	C–Zr	C–H- - -Zr
3-21G/CEP-31G	123.2	1.991	2.752
6-311G/SDD	123.5	1.981	2.744
6-311++G/SDD	123.5	1.982	2.745
6-311+G(2d)/SDD	97.1	1.963	2.373
6-311+G(2d,p)/SDD	95.5	1.960	2.345
6-311+G(2d, p)/SDD+G(3df)	95.4	1.961	2.345
6-311+G(2d, p)/LANL2DZ	94.2	1.956	2.320
6-311+G(3df)/SDD	94.0	1.955	2.319
6-311G(3df,3pd)SDD	92.9	1.955	2.300
6-311+G(3df,3pd)/SDD	92.9	1.955	2.300
6-311++G(3df,3pd)/SDD	92.9	1.955	2.300
6-311++G(3df,3pd)/SDD+G(3df)	93.1	1.955	2.303
6-311G(3df,3pd)/LANL2DZ	91.9	1.952	2.280
6-311++G(3df,3pd)/LANL2DZ	91.8	1.953	2.280
6-311++G(3df,3pd)/LANL2DZ+G(3df)	91.8	1.953	2.279

Table 5. Strongest Infrared Absorptions (cm^{-1}) Computed for $(CH_3)_2ZrH_2$[a]

$(CH_3)_2ZrH_2$	$(CD_3)_2ZrD_2$	$(^{13}CH_3)_2ZrH_2$
1663.0 (A, 319)[b]	1180.6 (166)	1663.0 (319)
1633.4 (B, 531)	1165.2 (276)	1633.4 (531)
1418.6 (B, 13)	1029.9 (9)	1415.5 (13)
1160.6 (B, 18)	914.7 (42)	1150.7 (15)
613.2 (A, 132)	473.7 (143)	612.4 (129)
566.5 (B, 251)	473.5 (70)	562.1 (246)

[a] 6-311++G(3df, 3pd) basis set. [b] Mode symmetry in C_s point group, infrared intensity in km/mol.

Similar calculations for CH_2═TiH_2 give agostic structures using both effective core potentials for Ti and even stronger agostic interaction using the all-electron basis for Ti.

A similar calculation was done for the lowest triplet CH_2−ZrH_2 state, which is 17.0 kcal/mol higher in energy, almost planar C_{2v} symmetry, with C−Zr, 2.200 Å; ∠HCZr, 125.0°; C−H- - -Zr, 2.966 Å, and no agostic interaction.

Calculations were also done for the CH_3ZrH and $(CH_3)_2ZrH_2$ molecules, and their structures are also presented in Figure 7. All frequencies were real, and CH_3ZrH has a $^3A''$ ground state and $(CH_3)_2ZrH_2$ has a ^1A ground state in C_2 symmetry. Important isotopic frequencies for $(CH_3)_2ZrH_2$ are given in Table 5. We have also calculated the agostic CH_2═ZrH_2- - -HCH_3 complex shown in Figure 7 and found it bound by 3.4 kcal/mol with H_3C−H- - -Zr distance of 2.243 Å. The "original" agostic C−H- - -Zr distance in CH_2═ZrH_2 is increased to 2.393 Å. The analogous CH_2═ZrH_2- - -Ar complex has the argon atom bound at 2.962 Å and 2.2 kcal/mol. Finally, Table 6 presents geometrical parameters and physical constants for the important Zr and CH_4 reaction products. The Mulliken charges reveal polarity with considerable negative charge on C and positive charge on Zr.

Table 6. Geometrical Parameters and Physical Constants Calculated for CH_2═ZrH_2, CH_3−ZrH, and $(CH_3)_2ZrH_2$

parameters[a]	CH_2═ZrH_2	CH_3−ZrH	$(CH_3)_2ZrH_2$
r(C−H_1)	1.115	1.094	1.093
r(C−H_2)	1.084	1.098	1.097
r(C−Zr)	1.955	2.216	2.212
r(Zr−H_3)	1.874		1.868
r(Zr−H_4)	1.884	1.873	1.868
<H_1CH_2	112.5	108.3	108.2
<$CZrH_3$	105.9		108.8
<$CZrH_4$	110.2	117.5	108.8
<H_3ZrH_4	116.4		111.5
<H_1CZr	92.9	112.9	114.6
<H_2CZr	153.5	109.7	108.9
Φ(H_1CZrH_4)	−142.8	0.0	119.1
Φ(H_2CZrH_4)	16.1	120.9	−119.5
symmetry	C_1	C_s	C_2
q(C)[b]	−0.78	−0.86	−0.96
q(H_1)[b]	0.02	0.03	0.06 (×2)
q(H_2)[b]	0.04	0.04	0.07 (×4)
q(H_3)[b]	−0.42	0.04	−0.43
q(H_4)[b]	−0.44	−0.46	−0.43
q(Zr)[b]	1.59	1.22	2.40
μ[c]	3.59	2.04	1.15
state[d]	^1A	$^3A''$	^1A
ΔE[e]	21.7	25.0	65.5

[a] Calculated at the B3LYP/6-311++G(3df, 3dp)/SDD level. Bond lengths and angles are in Å and deg. [b] Mulliken charges. [c] Dipole moment in D. [d] Electronic state. [e] Binding energies (kcal/mol) relative to Zr (^3F) + CH_4.

Discussion

The new product absorptions will be assigned to the simplest alkylidene hydride complex, zirconium methylidene, CH_2═ZrH_2, and its methane activation product, $(CH_3)_2ZrH_2$, on the basis of observed and calculated isotopic frequencies. The agostic bonding in CH_2═ZrH_2 will be documented. The unusual matrix effects observed for the reactive CH_2═ZrH_2 molecule will be considered.

CH_2═ZrH_2. The four new product absorptions marked 1 at 1581.0, 1546.2, 757.0, and 634.5 cm^{-1} in solid neon and the 1 and 1′ sets of bands in solid argon can be assigned to CH_2═ZrH_2. First, the 1581.0 and 1546.2 cm^{-1} bands shift to 1133.1 and 1112.3 cm^{-1} on deuteriation and exhibit 1.3953 and 1.3901 H/D ratios, which characterizes symmetric and antisymmetric Zr−H_2 stretching modes.[26] The ZrH_2 molecule has been observed at 1519 cm^{-1} in solid argon and at 1530 cm^{-1} in solid neon.[27,28] The cartesian displacement coordinates show that the stronger computed 1603.0 cm^{-1} mode is antisymmetric in

(26) The G matrix elements for symmetric and antisymmetric modes of a MH_2 group are different: $G_{sym} = \mu H + \mu M + \mu M \cos\alpha$ and $G_{antisym} = \mu H + \mu M - \mu M \cos\alpha$ where μ is the reduced (i.e., inverse) mass. Thus for 90° < α < 180°, the sym mode has less metal and hence more H participation.
(27) Chertihin, G. V.; Andrews, L. *J. Phys. Chem.* **1995**, *99*, 15004.
(28) Similar experiments with Zr and H_2 in excess neon give 1648 cm^{-1} for ZrH_4 and 1530 cm^{-1} for ZrH_2.

character, but the longer Zr−H bond (trans to the agostic H) stretches more than the shorter Zr−H bond (cis to the agostic H). These coordinates further show that the weaker computed 1633.7 cm^{-1} mode is symmetric in character and the shorter Zr−H bond stretches more than the longer Zr−H bond. The 757.0 cm^{-1} band shows a 19.6 cm^{-1} ^{13}C and a 70.0 cm^{-1} D shift, whereas the 634.5 cm^{-1} absorption exhibits 4.7 cm^{-1} ^{13}C and 135.1 cm^{-1} D shifts. These shifts characterize predominantly C═Zr stretching and CH_2 wagging modes, as will be shown later by comparison to calculated frequencies.

Our calculations predict that CH_2═ZrH_2 has the C_1 symmetry structure illustrated in Figure 7. The higher energy C_s and C_{2v} structures have imaginary frequencies and deform along the imaginary CH_2 rocking and ZrH_2 wagging modes to the more stable C_1 ground-state structure. Furthermore, the observed mixed H, D isotopic spectrum requires a low symmetry structure. Our calculations for CHD═ZrHD isotopic molecules show that the cis and trans isomers for C_{2v} and C_s structures give the same (±0.1 cm^{-1}) DZr−H and HZr−D stretching modes, but for the C_1 structure four isotopomers are possible (Chart 1), and these give rise to two distinct DZr−H and two distinct HZr−D stretching modes (Table 3), and four such bands are found (Figures 3 and 5). Our calculations describe four distinct CHD═ZrHD isotopmers (3, 4, 5, and 6 in Chart 1), and two of these have Zr−H and Zr−D stretching modes different from the other two. Our calculations predict 3 and 5 to have a Zr−H mode 7.8 cm^{-1} above the strong antisymmetric stretching mode of 1 and a Zr−D mode 14.2 cm^{-1} above the strong antisymmetric stretching mode of 8. These bands are observed 8.3 and 17.0 cm^{-1} higher, respectively. In a similar manner, our calculations find 4 and 6 to have strong Zr−H and Zr−D stretching modes 22.5 and 3.5 cm^{-1} above 1 and 8, and these bands are observed 24.8 and 4.0 cm^{-1} higher, respectively. The bands labeled 2 and 7 in Figure 5 due to CD_2═ZrH_2 and CH_2═ZrD_2 are predicted to shift 0.1 cm^{-1} from 1 and 8, and 0.7 and 0.2 cm^{-1} differences are found (Table 1). Finally, we note that the H(D) on Zr that is cis to the agostic H(D) has a higher frequency than the H(D) on Zr in the trans position, which further shows that the agostic interaction also discriminates between the two hydrides on zirconium.

In conclusion, the excellent agreement between experiment and theory for Zr−H and Zr−D stretching modes in four different CHD═ZrHD isotopomers (3, 4, 5, and 6) with H or D in the agostic bonding position confirms the identification and the C_1 symmetry agostic structure for CH_2═ZrH_2. Although CH_2═ZrH_2 has the same number of electrons in the valence shell with the fundamentally and industrially important symmetrical planar ethylene molecule, CH_2═CH_2, the d orbitals on Zr support agostic bonding to one methylene hydrogen and reduce symmetry in the CH_2═ZrH_2 molecule.

Additional spectroscopic evidence for the C_1 structure is found in the lower frequency C−Zr stretching and CH_2 wagging modes, whose vibrational character and thus isotopic shifts depend heavily on molecular symmetry. The C_1 structure has a strong mostly C−Zr stretching mode computed at 766.7 cm^{-1} (6-311++G(3df,3pd) basis set) with 18.0 cm^{-1} ^{13}C shift and 84.3 cm^{-1} D shift. A pure ^{12}C−Zr diatomic oscillator would shift 26 cm^{-1} for ^{13}C−Zr in this region. Hence, the observed 757.0 cm^{-1} absorption with 19.6 cm^{-1} ^{13}C shift and 70.0 cm^{-1} D shift fits the C_1 frequency prediction very well. Our calculation for the C_1 structure slightly underestimates the ^{13}C shift and overestimates the D shift for this mode. The strong CH_2 wagging mode is computed at 664.7 cm^{-1} for the C_1 structure. The associated absorption observed at 634.5 cm^{-1} is clearly in line with the calculation, and the isotopic shifts are appropriate for this assignment. The CH_2D_2 experiment revealed weak broad bands at 750 and 718 cm^{-1}, which contain C−Zr modes for the 3, 6 and 4, 5 CHD═ZrHD isomers, respectively.

The related satellite features at 1586 and 1551.0 cm^{-1} are due to a different neon packing configuration around CH_2═ZrH_2 that is formed on annealing and destroyed on photolysis. The stronger argon matrix interaction allows the second different packing configuration for CH_2═ZrH_2 in argon to make a more significant contribution to the spectrum and to exhibit a larger matrix shift. We noticed in argon matrix experiments that the 1 set (1504.3, 1553.9, 747.0, and 630.2 cm^{-1}) increased much more on $\lambda > 530$ nm irradiation than the 1′ set (1524.8, 1557.8, 759.8, and 652.6 cm^{-1}), but UV (240−380 nm) irradiation increased the 1′ set and decreased the 1 set. This photoreversible process was persistent for up to four cycles. The argon matrix frequencies are just below the neon matrix frequencies for CH_2═ZrH_2, and they can be assigned accordingly to CH_2═ZrH_2 in two different argon matrix packing configurations. In this regard we compute that an argon atom binds at a 2.962 Å distance above Zr with a 2.2 kcal/mol binding energy. We suspect that the reversible photochemistry involves the triplet upper state, which has a nearly planar structure and a different argon matrix cage arrangement, and on relaxation to the singlet state, retains that different argon cage arrangement.

The 1 bands at 1553.9 and 1504.3 cm^{-1} in solid argon shift to 1082.4 and 1115.3 cm^{-1} on deuteriation and exhibit 1.3968 and 1.3898 H/D ratios, and in a similar manner the 1′ bands at 1557.8 and 1524.8 cm^{-1} shift to 1115.3 and 1097.3 cm^{-1} with 1.3983 and 1.3896 H/D ratios. As for the neon matrix observations, the 1 and 1′ bands are due to symmetric and antisymmetric Zr−H_2 stretching modes. The 747.1 and 630.2 cm^{-1} absorptions are assigned to the mostly C═Zr stretching and CH_2 wagging modes for 1 with analogous 759.8 and 652.6 cm^{-1} bands for 1′. Note that the isotopic shifts are slightly different in solid argon as the matrix interaction alters mode mixing as well as position. Note also that the neon matrix bands for these modes contain both neon matrix sites, which fall between the two argon matrix site absorptions.

Although the argon matrix spectra for the Zr reaction with CH_2D_2 are more complicated, two sets of CHD═ZrHD absorptions are observed in the Zr−H stretching region for 1 and 1′ sites (Table 1, footnotes d and e) and two sets are observed for the 1′ site (footnote g) in the Zr−D stretching region where CH_2D_2 absorption covers the 1 bands. The displacements are comparable to those observed in solid neon. With the larger methylidene complex yield in solid argon, more information on CHD═ZrHD isomers is available in the lower frequency region, and such bands are given in Table 1. The 733 and 702 cm^{-1} bands can be assigned to the 3, 6 and 4, 5 CHD═ZrHD isotopomers in the first matrix configuration formed on $\lambda >$ 530 nm irradiation.

$(CH_3)_2ZrH_2$. The strong 1617.2 and 1587.5 cm^{-1} absorptions (labeled "di" in Figure 4) are assigned to dimethyl zirconium dihydride, $(CH_3)_2ZrH_2$. These frequencies may be compared to the antisymmetric stretching mode for ZrH_4 observed at 1623

cm^{-1} in solid argon and at 1648 cm^{-1} in solid neon.[27,28] Our calculations predict a very stable molecule with C_2 symmetry and strong Zr−H_2 stretching modes at 1663.0 and 1633.4 cm^{-1}, which are only 2.9% higher than the observed values and in line with other comparisons for stable molecules containing first-row transition-metal atoms.[29] The $(CD_3)_2ZrD_2$ counterparts at 1158.1 and 1142.6 cm^{-1} and single intermediate −ZrHD species bands at 1602.2 and 1150.5 cm^{-1} confirm this assignment. The H/D frequency ratios 1.3964 and 1.3896 are appropriate for symmetric and antisymmetric Zr−H_2 stretching modes[26] as described by the calculation. The next strongest lower frequency ZrH_2 bending and deformation modes predicted at 613.2 and 566.5 cm^{-1} are observed here at 593.4 and 564.2 cm^{-1}, and weaker CH_3 bending and deformation modes computed at 1418.6 and 1160.6 cm^{-1} are found at 1375.1 and 1125.0 cm^{-1}. The ^{13}C shifts for these modes are predicted as 3.1, 9.9, 0.8, and 4.4 cm^{-1} and observed as 3.1, 10.2, 1.2, and 5.0 cm^{-1}. The argon matrix bands at 1603.1 and 1572.6 are likewise due to $(CH_3)_2ZrH_2$. The deuterium shifts to 1147.7 and 1131.5 cm^{-1}, and H/D ratios 1.3968 and 1.3898 and single −ZrHD intermediate bands at 1587.6 and 1140.0 cm^{-1} support this assignment. This is the first report of a group 4 dimethyl dihydride, which is an interesting molecule in its own right. The $(CH_3)_2TiF_2$ analogue has been observed in similar Ti reactions with CH_3F,[12] and $(CH_3)_2TiCl_2$ is an isolatable molecule.[30]

CH_3ZrH. The CH_3ZrH insertion product that precedes CH_2═ZrH_2 has yet to be identified. Our B3LYP calculations predict one strong absorption at 1604 cm^{-1}, the same position as the strongest CH_2═ZrH_2 band. However, the $^3A''$ state CH_3ZrH molecule is likely to interact more strongly with the matrix cage than singlet CH_2═ZrH_2, and CH_3ZrH is expected to absorb just below CH_2═ZrH_2. A weak 1533.5 cm^{-1} band produced on irradiation with Zr and CH_4 in solid neon sharpens on annealing. This band shows no ^{13}C shift, and the 1096.8 cm^{-1} band with CD_4 exhibits the same behavior. This 1.3982 H/D ratio is appropriate for a symmetric Zr−H stretching vibration. The CH_2D_2 experiment reveals a similar band at 1533.2 cm^{-1}. Similarly weak 1496.2 and 1488.4 cm^{-1} bands formed on irradiation of Zr and CH_4 in solid argon sharpen and decrease on annealing and shift to 1077.1 and 1071.7 cm^{-1} with CD_4, and CH_2D_2 gives similar bands at 1496.1 and 1488.1 cm^{-1}. The H/D ratios 1.3891 and 1.3888 are slightly lower for this species in the more strongly interacting argon matrix. We also note that the relative yield of the deuterated product is higher in both matrixes and that the yield of this product relative to the methylidene complex is higher in solid argon than solid neon.

These bands appear to be due to CH_3ZrH, although an identification based on a single band is not as definitive as those based on four or six fundamental frequencies.

Reaction Mechanisms. The zirconium atom reaction with methane apparently proceeds with excited Zr atoms produced in the laser ablation process[20] or by irradiation[31] as C−H activation to form the CH_3ZrH intermediate requires activation energy.[18] The excited intermediate thus formed can be relaxed by the matrix or undergo α-hydrogen transfer[32] to give first the higher energy triplet CH_2−ZrH_2 and then singlet CH_2═ZrH_2 (eq 1). It is in this intermediate triplet state that CHD−ZrHD isotopomers partition into the four possible forms (Chart 1). Our calculations show that CH_3ZrH ($^3A''$) and CH_2═ZrH_2 (^1A) have comparable energies (Table 6).

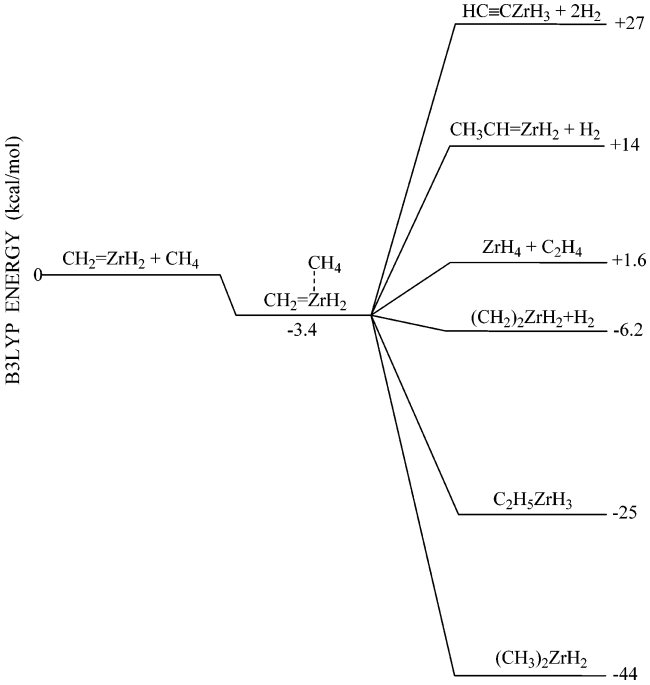

Figure 8. Relative energies of CH_2═ZrH_2 + CH_4 reaction products computed at the B3LYP/6-311++G(3df, 3pd)/SDD level.

$$Zr^* + CH_4 \rightarrow [CH_3ZrH]^* \xrightarrow{\text{relax}} CH_3ZrH \qquad (1a)$$

$$Zr^* + CH_4 \rightarrow [CH_3ZrH]^* \rightarrow [CH_2{-}ZrH_2]^* \rightarrow CH_2{=}ZrH_2 \qquad (1b)$$

$$CH_2{=}ZrH_2 + CH_4 \rightarrow (CH_3)_2ZrH_2 \qquad (2)$$

However, the reaction with a second CH_4 molecule to form $(CH_3)_2ZrH_2$ appears to be spontaneous on annealing in solid neon based on the slight increase in the latter product absorptions (Figure 4). The $(CH_3)_2ZrH_2$ molecule is computed to be 65 kcal/mol more stable than Zr (^3F) and two methane molecules, and eq 2 is exothermic by 44 kcal/mol. Alkylidene complexes are also known for C−H activation,[2] and eq 2 provides a simple example of the important C−H activation process for methane. The first step in the CH_2═ZrH_2 reaction with CH_4 is formation of the CH_2ZrH_2−CH_4 complex. The positive Zr in CH_2═ZrH_2 is the center for attracting H from CH_4, and the optimized complex structure (Figure 7) is bound by 3.4 kcal/mol, which serves as the precursor to $(CH_3)_2ZrH_2$. Recall that CH_4 and CD_4 together gave the Me_2ZrHD product so it appears that H addition to the Zr center occurs before reverse hydrogen migration and methyl attachment. The relative energies of several CH_2═ZrH_2 plus CH_4 reaction products are displayed in Figure 8: The $(CH_3)_2ZrH_2$ molecule lies lowest in energy, but $C_2H_5ZrH_3$ might also be observable. The HC≡$CZrH_3$ molecule found in recent Zr/C_2H_4 investigations[23] was not detected here.

(29) Bytheway, I.; Wong, M. W. *Chem. Phys. Lett.* **1998**, *282*, 219.

(30) McGrady, G. S.; Downs, A. J.; Bednall, N. C.; McKean, D. C.; Thiel, W.; Jonas, V.; Frenking, G.; Scherer, W. *J. Phys. Chem. A* **1997**, *101*, 1951 and references therein.

(31) A host of Zr* metastable states are observed below 2 eV: Moore, C. E. *Atomic Energy Levels*; Circular 467; National Bureau of Standards: Washington, DC, 1952.

(32) Crabtree, R. H. *The Organometallic Chemistry of the Transition Metals*; Wiley and Sons: New York, 2001; p 190.

Some mechanistic information can be obtained from the CH_2D_2 experiments. In the neon matrix experiments, the 1545.5 cm^{-1} $CD_2{=}ZrH_2$ absorption is double the intensity of the 1112.5 cm^{-1} band for $CH_2{=}ZrD_2$, and since computed infrared intensities are 2/1 (Table 3) these two isomers are produced in essentially the same yield. This suggests that there is no preference for insertion by Zr into a C−H or C−D bond in the same molecule nor is there a preference for α-H over α-D transfer to Zr. Statistically, then, CHD═ZrHD isotopomers 3, 4, 5, and 6 are equally probable, but our spectra show a clear (approximately 2/1) preference for 3, 5 over 4, 6, based on DZr−H and HZr−D stretching band absorbances normalized by calculated infrared intensities for each pair. How can we rationalize this preference? Each pair contains one isotopomer with H and one with D in the elongated C−H(D) agostic bonding position so that is not the deciding factor: there appears to be no isotopic preference for the agostic bonding position. However, 3 and 5 both have Zr−D closer to the agostic bond (H or D), whereas 4 and 6 have Zr−H nearer to the agostic bond. We suggest that the larger vibrational amplitude associated with the Zr−H out-of-plane wagging motion interferes more with the agostic bond, and the CHD−ZrHD triplet state initially formed by α-transfer partitions more into isomers 3 and 5 as opposed to 4 and 6. We cannot determine the 3 vs 5 distribution, but we note that 5 has the lowest zero point energy of all CHD═ZrHD forms, and we suspect that more of isotopomer 5 is trapped in the matrix. For comparison we include computed zero point energies for all of the $ZrCH_2D_2$ isotopomers in Table 3.

On the other hand, this neon matrix investigation with CH_2D_2 produces Me_2ZrH_2 and Me_2ZrHD in approximately equal yields but Me_2ZrD_2 at roughly 20% of the above isotopic forms. In addition, an argon matrix experiment with equimolar CH_4 and CD_4 reagents gives equimolar $CH_2{=}ZrH_2$ and $CD_2{=}ZrD_2$ primary products without CHD═ZrHD and the three above secondary dihydride products isotopomers in a 6/4/4 ratio, respectively. What does this information suggest about the mechanism of eq 2? First, the observation of Me_2ZrHD from CH_4 and CD_4 with only $CH_2{=}ZrH_2$ and $CD_2{=}ZrD_2$ primary products present indicates that CH_3 (or CD_3) radical does not add first to the Zr center, hence H (or D) must. We suggest that the second methane is attracted to vacant d orbitals on Zr by agostic interaction.

Other Products. The neon matrix experiments with methane reveal weak 1648.2 and 1633.5 cm^{-1} bands that agree very well with major 1648.2 and 1633.7 cm^{-1} products in the analogous Zr experiment with H_2.[28] These bands show no shift with $^{13}CH_4$, but the major band shifts to 1184.6 cm^{-1} with CD_4 and both bands are observed with the CH_2D_2 precursor. The weak 518.9 cm^{-1} band is appropriate for the bending mode. Hence, the 1648.2 and 518.9 cm^{-1} absorptions can be assigned to ZrH_4, and this observation invites consideration of reactions to generate ZrH_4 from methane.

The stable hydrocarbons C_2H_2, C_2H_4, and C_2H_6 are observed in trace quantities in these experiments, and these are expected from high energy irradiation of methane in the laser-ablation process. The methyl radical[25] is also observed, particularly in the high concentration experiments. These absorptions are, of course, much stronger in the pure methane experiments where broad bands for ZrH_4 are also stronger.

The neat methane experiment also contains zirconium reaction products. The 1557 and associated 1594 cm^{-1} absorptions behaved on photolysis and annealing like the 1603.1 and 1572.6 cm^{-1} argon matrix absorptions for $(CH_3)_2ZrH_2$. A 547 cm^{-1} band is also associated with the latter molecule. This observation raises the question of $CH_2{=}ZrH_2$ trapping in solid methane, and weak 1545 and 1492 cm^{-1} bands decrease on photolysis and annealing while the above $(CH_3)_2ZrH_2$ absorptions increase. We tentatively assign the 1545 and 1492 cm^{-1} bands to $CH_2{=}ZrH_2$ trapped in solid methane. The 1503 and 1464 cm^{-1} bands remain to be identified: the CD_4 counterparts at 1088 and 1056 cm^{-1} suggest strongly that these absorptions arise from Zr−H stretching modes. The observation of ZrH_2 at 1519 cm^{-1} in solid argon suggests a similar species for the 1503 cm^{-1} absorption. Finally, the 1464 cm^{-1} band is probably due to another −ZrH species, and since the behavior parallels that described above for CH_3ZrH, this initial reaction product is a likely possibility. The more strongly interacting methane matrix may be more effective in stabilizing CH_3ZrH.

Conclusions

Reaction of laser-ablated Zr with CH_4 ($^{13}CH_4$, CD_4, and CH_2D_2) in excess neon during condensation at 5 K forms $CH_2{=}ZrH_2$, the simplest carbene hydride complex, which is identified by infrared absorptions at 1581.0, 1546.2, 757.0, and 634.5 cm^{-1}. Density functional theory electronic structure calculations using a large basis set with polarization functions, particularly on carbon, predict a C_1 symmetry structure with agostic C−H- - -Zr bonding and distance of 2.300 Å. Identification of the agostic $CH_2{=}ZrH_2$ methylidene complex is confirmed by an excellent match of calculated and observed isotopic frequencies particularly for the four unique CHD═ZrHD isotopic modifications. The analogous reactions in excess argon give two sets of infrared bands for persistent photoreversible matrix configurations for $CH_2{=}ZrH_2$. The $CH_2{=}ZrH_2$ complex is an excellent model for examination of the intramolecular agostic bonding interaction especially in view of a recent definition of agostic bonding.[33]

Methane activation by $CH_2{=}ZrH_2$ gives the new $(CH_3)_2ZrH_2$ molecule, which is identified by six fundamental frequencies and is the most stable molecule for this stoichiometry.

Acknowledgment. We gratefully acknowledge financial support for this work from N.S.F. Grants CHE 00-78836 and CHE 03-52487, sabbatical leave support (H.-G. Cho) from the Korea Research Foundation (KRF-2003-013-C00044), and helpful suggestions from C. W. Bauschlicher, Jr.

JA0451259

(33) Scherer, W.; McGrady, G. S. *Angew. Chem. Int. Ed.* **2004**, *43*, 1782.